



## PH-17

### Enhancement of the Magnetic Properties of Ni-Cu-Zn Ferrites by the Non-magnetic Al<sup>3+</sup>-ions Substitution

M. M. Eltabey, K.M. El-Shokrofy and S.A. Gharbia

#### Abstract

The effect of Al-substitution on the physical, magnetic and electrical properties of Ni-Cu-Zn ferrite of chemical formula  $Ni_{0.4}Cu_{0.2}Zn_{0.4}Al_xFe_{2-x}O_4$  ( $x = 0$  to  $x = 0.15$  with step = 0.025) which prepared by conventional ceramic method has been studied. X-ray patterns indicated the presence of a single spinel phase. The magnetization is measured using VSM at room temperature. The initial permeability is measured, on toroidal samples used as transformer cores, as a function of temperature at constant frequency of 10 KHz and Curie temperature is determined. It was found that Al-ion substitute improved the magnetization as well as the initial permeability. The dc resistivity is also increased with increasing Al – concentration. Such results are promising ones for the high frequency applications.

#### 1- Introduction:

Ferrites are very important in technological applications as inductor cores because they have high resistivity compared to metallic materials. The magnetic properties of ferrites such as the permeability, magnetization and coercive field are affected by the type of the substituted ion, microstructure and the porosity [1]. The miniaturization trend of electronic devices results in the rapid development of surface mount devices (SMD) [23]. As one of the most important SMD, multilayer chip inductors (MLCI) become more and more miniaturized and integrated [4]. Ni-Cu-Zn ferrite is one of the soft magnetic materials which is used for MLCI applications because of their relatively low sintering temperature, high permeability in the R-F frequency region and high electrical resistivity [5, 6]. The effect of substituting trivalent ions for iron in ferrites has been investigated [7, 8]. Samy et al. studied the effect of substitution of Nd for iron in the system  $Cu_{0.5}Zn_{0.5}Nd_xFe_{2-x}O_4$  and they found that the sample with  $x=0.02$  improves the magnetization, the relative permeability and the initial permeability [9]. Sankpal et al.[10] studied the effect of substitution of Al for iron in the system  $Ni_{0.7}Zn_{0.3}Al_xFe_{2-x}O_4$  and they found that the thermal variations of remanence ratio R and coercive field  $H_c$  reveal that this composition contains predominantly multidomain (MD) grains. With the substitution of Al<sup>3+</sup>, the saturation magnetization  $M_s$  and R decrease. The decreasing behavior is explained on the basis of exchange interaction and the effect of the anisotropy constant  $K_1$ . In the present study, the effect of Al<sup>3+</sup>-ions substitution on the

physical, magnetic and electrical properties of  $\text{Ni}_{0.4} \text{Cu}_{0.2} \text{Zn}_{0.4} \text{Al}_x \text{Fe}_{2-x} \text{O}_4$  ferrites will be studied.

## 2-Experimental procedure:

Samples with the chemical formula  $\text{Ni}_{0.4} \text{Cu}_{0.2} \text{Zn}_{0.4} \text{Al}_x \text{Fe}_{2-x} \text{O}_4$  ( $x = 0$  to  $x = 0.15$  with step = 0.025) were prepared by using standard ceramic technique. High purity oxides, 99.9% of NiO, CuO, ZnO,  $\text{Al}_2\text{O}_3$  and  $\text{Fe}_2\text{O}_3$  were mixed together according to their molecular weights. The mixture of each sample was ground to a very fine powder and then presintered at  $900^\circ\text{C}$  for 12 h in one cycle. The presintered mixture was ground again and pressed at room temperature into discs and toroids. They were finally sintered at  $1200^\circ\text{C}$  for 5h and then slowly cooled at room temperature. X-ray diffraction (XRD) patterns were formed using diffractometer of type x'pert Graphics identify with  $\text{CuK}\alpha$  radiation. The porosity percentage (P %) was calculated for all samples according to the relation  $P\% = 100 [1 - (d/d_x)] \%$ . Where  $d_x$  is the theoretical x-ray density of samples which calculated using the formula  $d_x = 8M/\text{Na}^3$  (M is the molecular weight, N is Avogadro's number and a is the lattice parameter) and d is the density of each composition measured in water using Archimedes principle. The magnetization M (emu/g) is measured at room temperature in the magnetizing field H (Oe) ranged from zero to 6000 Oe using the LDJ vibrating sample magnetometer (VSM) model 9600. The initial permeability ( $\mu_i$ ) was measured as a function of temperature at constant frequency ( $f = 10$  kHz) and low magnetizing current of  $I_p = 10$  mA. The value of  $\mu_i$  was calculated using poltinnikov's formula [11], which is given by  $V_s = K\mu_i$ ,  $K = 0.4\pi N_p N_s I_p A \omega / L$  where  $V_s$  is the induced voltage in secondary coil,  $N_p$  and  $N_s$  are the number of turns of primary and secondary coils, respectively ( $N_p = N_s = 20$  turns). A is the cross – sectional area of the sample,  $\omega$  is the angular frequency ( $\omega = 2 \pi f$ ) and L is the average path of magnetic flux ( $L = 2 \pi r_m$ ) where  $r_m$  is the mean radius of toroid.

## 3- Results and Discussion

### 3.1 Physical Properties:

The XRD patterns in Fig. (1) indicate that all investigated samples formed in cubic single spinel phase. The values of d-spacing are calculated according to Bragg's law and hence the average lattice parameter a (Å) is calculated. The variation of a (Å) with the Al-concentration is plotted in

Fig. (2). It is clear that as Al-concentration increases the lattice parameter decreases almost linearly obeying Vegard's law. Similar behavior was observed in Al-substituted Mn-Zn [12, 13], Ni-Zn [14] and Mn-Ni-Zn ferrites [15]. The decrease in lattice parameter with increasing Al-concentration could be explained on the basis of the ionic radii due to the replacement of ions with larger ionic radius of  $\text{Fe}^{3+}$  (0.64Å) by the smaller one  $\text{Al}^{3+}$  (0.51Å).

The variations of porosity and the grain size with Al-concentration are shown in table (1). It is obvious that, as Al-concentration increases the porosity increases up to  $x=0.05$  and then decreases. This behavior could be explained as following: It is known that the porosity of ceramic samples results from two sources intragranular porosity ( $P_{\text{intra}}$ ) and intergranular porosity ( $P_{\text{inter}}$ ) [16]. Thus, the total porosity could be written as the sum of two types i.e.,

$$P = P_{\text{intra}} + P_{\text{inter}} \quad (1)$$

Furthermore, it was reported that the intergranular porosity ( $P_{\text{inter}}$ ) is directly proportional to the grain size [17, 18]. It is found that, see table (1), as Al-concentration increases the grain size increases up to  $x = 0.05$  and then decreases. From this behavior one can observe that the behavior of D,  $P_{\text{inter}}$  and P% are the same. Thus according to equation (1), one could be

concluded that the total porosity P (%) for these samples results mainly from the intergranular porosity ( $P_{inter}$ ).

### 3. 2 Magnetic Properties

#### 3. 2. 1 Magnetization:

The variation of magnetization M (emu/g) with applied magnetic field H (Oe) for all investigated samples at room temperature is shown in Fig.(3). As a normal behavior, the magnetization increases with increasing applied magnetic field and attain its saturation value for higher fields. The dependence of saturation magnetization ( $M_s$ ) on Al-concentration is shown in Fig.(4). It is clear that ,as Al-concentration increases  $M_s$  increases up to its maximum value at  $x=0.05$ , with percentage increase  $\Delta M_s \% = 6.9 \%$  as shown in table (1), and then decreases. This could be explained as following: It is known that, for Ni-Zn and Cu-Zn ferrites there is a canting angle, Yafet-Kittel angle ( $\alpha_{YK}$ ), between moments in B-site at Zn concentration=0.4. Such a canting angle is due to the negative B-B interaction [19, 20] .Thus, the total magnetization could be expressed as:

$$M=M_B \cos \alpha_{YK} - M_A \quad (2)$$

Where  $M_A$  and  $M_B$  are the magnetic moments of A and B-sites respectively [21]. According to that equation, the increase of  $M_s$  up to  $x=0.05$  with increasing Al-concentration can be attributed to the increase of  $\cos \alpha_{YK}$  i.e. decreasing of  $\alpha_{YK}$  due to the decrease of the negative B-B interaction leading to enhancing the parallelism of moments in B-site . For  $x>0.05$ , i.e. further replacement of the magnetic  $Fe^{3+}$ -ions by non magnetic  $Al^{3+}$ -ions in B-site leads to decrease of the magnetic moment of B-site and hence the total magnetization have to decrease.

#### 3.2.2 Initial Permeability and Curie Temperature:

Fig. (5) shows the variation of the initial permeability ( $\mu_i$ ) with temperature T(k) for all samples. It is found that the curves are typical of multi domain grains showing a sudden drop in  $\mu_i$  at the Curie temperature ( $T_c$ ). It is determined by drawing a tangent for the curve at the rapid decrease of  $\mu_i$ . The intersection of the tangent with T-axis determines  $T_c$ . It was reported that the sharp decrease of  $\mu_i$  with temperature at  $T_c$  reflects the homogeneity of the sample which can be expressed as  $(\Delta \mu_i / \Delta T)$  at  $T_c$  [22, 23]. It is known that the increase of the grain size occurs at the expense of the grain boundaries i.e. samples with larger grain size expected to be more homogenous. One can note that the sample with  $x=0.05$  has the maximum  $\Delta \mu_i / \Delta T$  and maximum grain size which confirms the later statement. The dependence of both the initial permeability  $\mu_i$  at room temperature and  $T_c$  on the Al-concentration are shown in Fig. (6). It is clear that, as Al-concentration increases  $\mu_i$  increases up to its maximum value at  $x = 0.05$ , with percentage increase  $\Delta \mu_i \% \approx 96\%$  as shown in table (1), and then decreases. The similarity in behavior of  $\mu_i$ , D and  $M_s$  with Al- concentration could be understood in view of the approximate equation for initial permeability [1].

$$\mu_i \cong \left( M_s^2 D / \sqrt{K_1} \right) \quad (3)$$

where  $M_s$ ,  $K_1$  and D are saturation magnetization, the anisotropy constant and the average grain size respectively. It is known that the anisotropy field in ferrites results from the presence of  $Fe^{2+}$ - ions which formed during the sintering process [24, 25]. Therefore, the replacement of  $Fe^{3+}$ - ions by  $Al^{3+}$ - ions leads to decrease the anisotropy constant, with increasing the Al-concentration , due to the relative reduction in  $Fe^{2+}$ - ion concentration. The increase of  $\mu_i$  with Al-concentration up to  $x=0.05$  is attributed to the increase of  $M_s$  and D with the decrease of  $K_1$ . While in the range of  $x>0.05$ , it is clear that the value of  $\mu_i$  decreases

with increasing Al-concentration. This means that the decrease of both  $M_s$  and  $D$  with Al-concentration in that range have the dominant effect.

Fig.(6) shows also that there is no considerable change in curie temperature with increasing Al-concentration. This constancy could be explained in the light of pair model. Where, the main factor that affects the value of  $T_c$  is the A-B interaction [19]. The constancy of  $T_c$  could be attributed to a competition between two factors: First, the decrease in the distance between the moments of A and B sites as noted from lattice parameter leads to increase of A-B interaction and hence  $T_c$  has to increase. On the other hand, due to the replacement of the magnetic  $Fe^{3+}$  -ions by the non magnetic  $Al^{3+}$  -one, the A-B interaction have to decrease leading to decrease  $T_c$ .

### 3.3 Electrical Resistivity:

The dependence of dc electrical resistivity ( $\rho$ ) at room temperature on Al-concentration is shown in Fig.(7). It is clear that, as Al-concentration increases the resistivity increases. Similar behavior was reported for Al-substituted ferrites [26-28]. This behavior of  $\rho$  could be attributed to the decrease of  $Fe^{2+}$  and  $Fe^{3+}$ -ions concentrations with increasing the Al-concentration. This leads to limit the hopping probability between  $Fe^{3+}$  and  $Fe^{2+}$ -ions.

### 4-Conclusion:

The lattice parameter decreased while the porosity increased with  $Al^{3+}$ -ion substitution in Ni-Cu-Zn ferrites. Al-ion substitution in that ferrite improved the saturation magnetization, the initial permeability and dc resistivity while Curie temperature approximately didn't affected.

### References:

- [1] G. C. Jain, B.K. Das, R.S. Khanduja, and S.C. Gupta, J. Mater. Sci. 11 (1976) 1335-1338 .
- [2] I. Z. Rahman, T. T. Ahmed, J. Magn. Magn. Mater. 290-291 (2005) 1576.
- [3] C. W. Kim, J. G. Koh, J. Magn. Magn. Mater. 257 (2003) 355.
- [4] B. Li, Z. X. Yue, X. W. Qi, J. Zhou, Z. L. Gui, L. T. Li, Mater. Sci. Engg. B 99 (2003) 252.
- [5] K. O. Low, F. R. Sale, J. Magn. Magn. Mater.246 (2002) 30-35.
- [6] H. I. Hsiang, W. C. Liao, Y. J. Wang, Y. F. Cheng, J. Euro. Ceram. Soc. 24 (2004) 2015-2021.
- [7] K. P. Belove, L. A. Antoshina, and A. S. Moreosyan, Sov. Phys. –Solid State 25 (1993) 1609.
- [8] M. A. Ahmed, Tawfik, EL-Nimr, and EL-Hasab, J. Mater. Sci. 10 (1991) 549.
- [9] A. M. Samy, H. M. El-Sayed, and A. A. Sattar, J. Phys.Stat. Sol. (a) 200, No. 2 (2003) 401-406.
- [10] A. M. Sankpal, S. S. Suryawanshi, S. V. Kakatkar, G. G. Tengshe, R. S. Patil, N. D. Chaudhari, S. R. Sawant, J. Magn. Magn. Mater.186 (1998) 349-356.
- [11] S. S. Poltinnikov and H. Turkevic, Sov. Phys-Solid state 8 (1966) 1144.
- [12] Chandrase Karan, G. S. selvandan and K. Manivannane, J. Mater Sci.: Materials in Electronics, 15 (2004) 15 – 18.
- [13] Kakatkar, S. V., S.S. Kakatkar, R. S. Patil, P.K. Maskar, A.M. Sankapal, S.S. suryawanshi, N.D. Chaudhari and S.R. Sawant, J. Mag. Mate. 159 (1996) 361 – 366.

- [14] Chandra, P. J. Mater. Sci. Lett. 6 (1987) 651 – 652.
- [15] A. A. Sattar, H. M. El-Sayed, K. M. El-Shokrofy and M. M. El-Tabey, J. Applied Sciences 5(1) (2005) 162-168.
- [16] Kigery, W.D., H.K. Bowen, D.R. Uhlmann, Introduction of ceramics published by John Wiley and sons New York, London, and P. P. (1975) 458.
- [17] Rezlescu, N. E. Rezlescu, C. Pasnicu and M.L. Graus, J. Phys. Condens. Matter, 6 (1994) 5707.
- [18] R.G. Kulkarni and V.U. Patial, J. Mater. Sci. 17(1982) 843 – 848.
- [19] ChikaZumi, S. and S. Charap, Physics of Magnetism. Published by John Wiley and Sons, Inc., New York, London, Sydney, (1964) 93.
- [20] Suryawanshi, S. S., V. Deshpand and S.R. Sawant, J.Mate.Chem.Phys, 59 (1999) 199-203.
- [21] Cedillo E.Ocampo J. and Rioera V. J. Phys. E: Sci.Instrum., 13 (1980) 383.
- [22] Sattar, A. A., Wafik A. H., K. M. El-Shokrofy, and M.M.El-Tabey: Phys.Stat.Sol. (a) 171 (1999) 563.
- [23] Sattar A. A., Samy A. M., J. Mater. Sci., 37 (2002) 449.
- [24] ChikaZumi, S. and S. Charap, Physics of Magnetism. Published by John Wiley and Sons, Inc., New York, London, Sydney, (1964) 153.
- [25] E.W. Gorter, Philips Res. Rep. 9 (1954) 295.
- [26] Abo El Ata A. M., Attia S. M. and Meaz T. M., J. Solid Stat. Sci., 6 (2004) 61.
- [27] Chandra Prakash, J. Mater. Sci., Letters, 6 (1987) 651.
- [28] Mason T. O. and Bowen H. K., J. Am. Ceram. Soc. 64 (1981) 237.

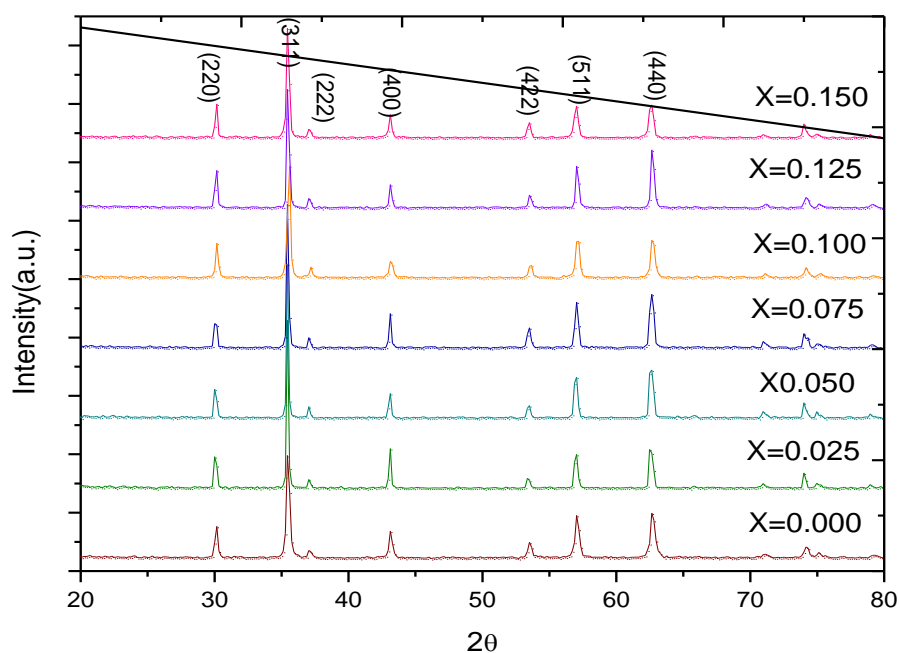


Fig. (1): X-ray diffraction pattern of  $\text{Ni}_{0.4}\text{Cu}_{0.2}\text{Zn}_{0.4}\text{Al}_x\text{Fe}_{2-x}\text{O}_4$

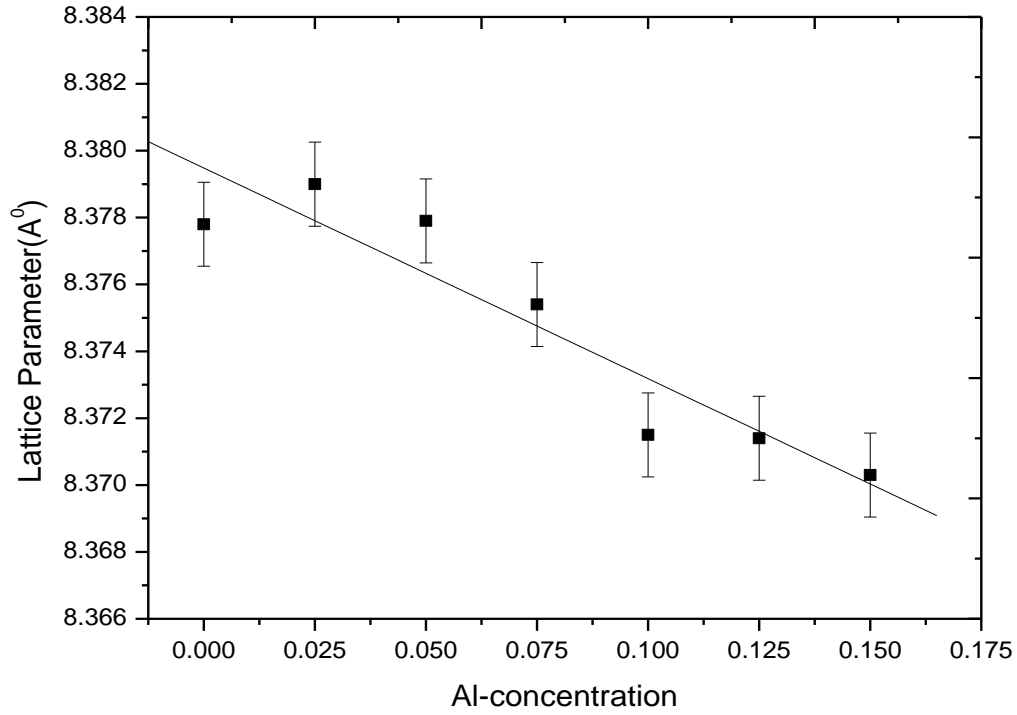


Fig.(2): Variation of lattice parameter  $a$  (Å) with Al-concentration

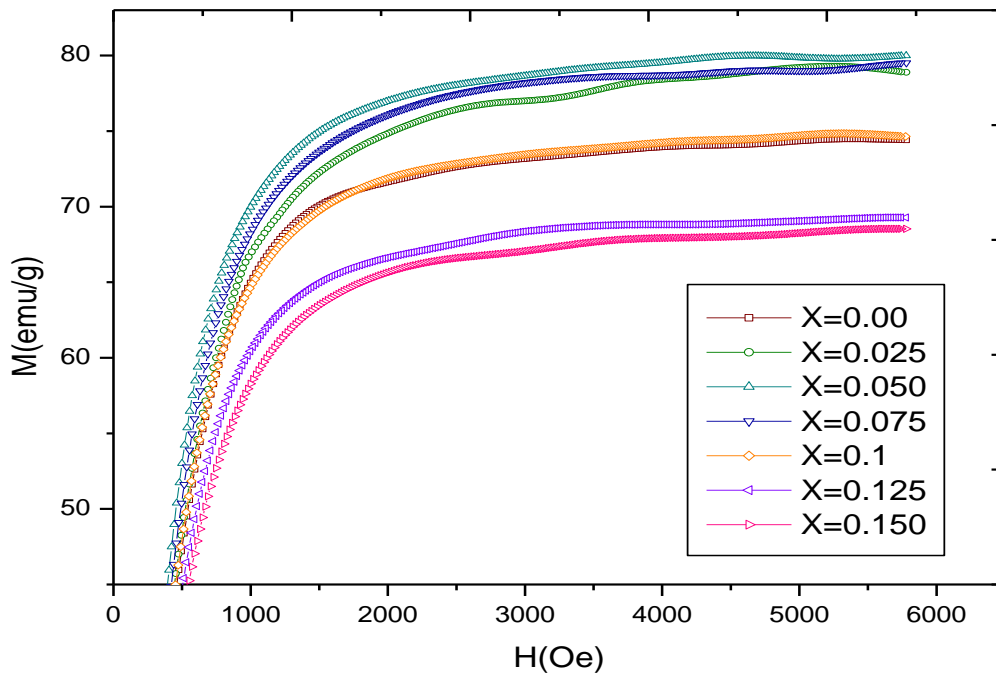


Fig.(3): Variation of magnetization  $M$  (emu/g) with  $H$  (Oe) for  $\text{Ni}_{0.4}\text{Cu}_{0.2}\text{Zn}_{0.4}\text{Al}_x\text{Fe}_{2-x}\text{O}_4$

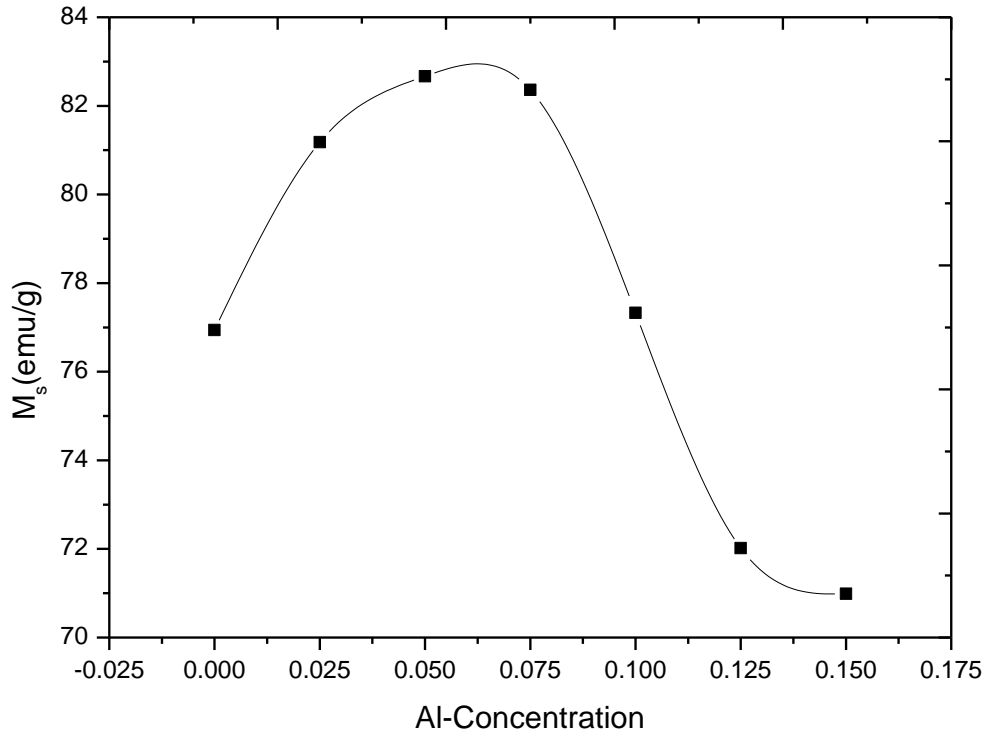


Fig.(4):

Variation of saturation magnetization  $M_s$ (emu/g) with Al-concentration

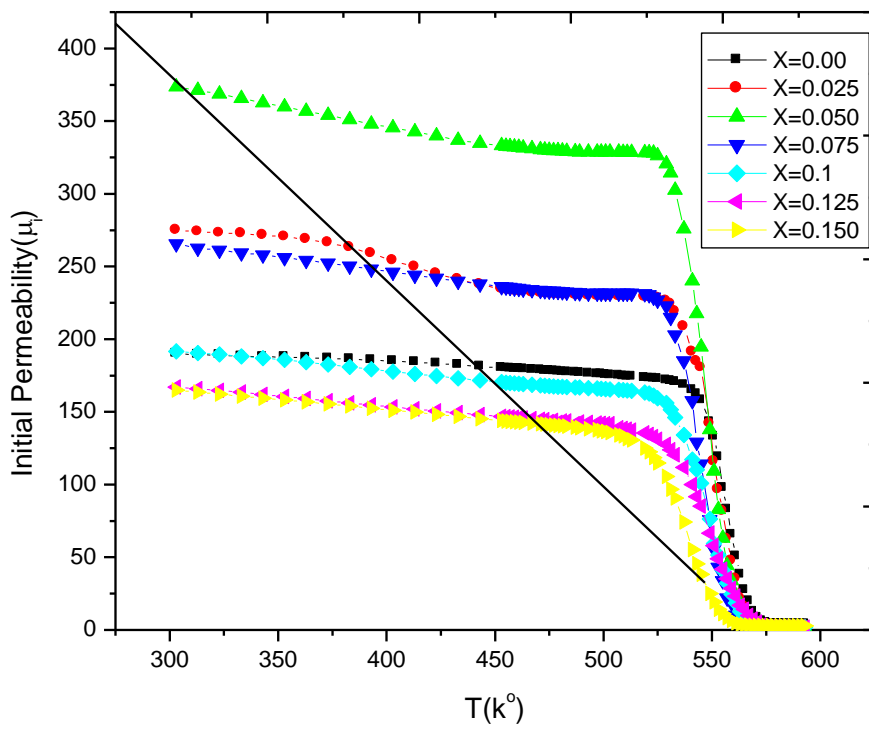


Fig (5): variation of the initial permeability ( $\mu_i$ ) with Temperature T(k) of  $\text{Ni}_{0.4}\text{Cu}_{0.2}\text{Zn}_{0.4}\text{Al}_x\text{Fe}_{2-x}\text{O}_4$

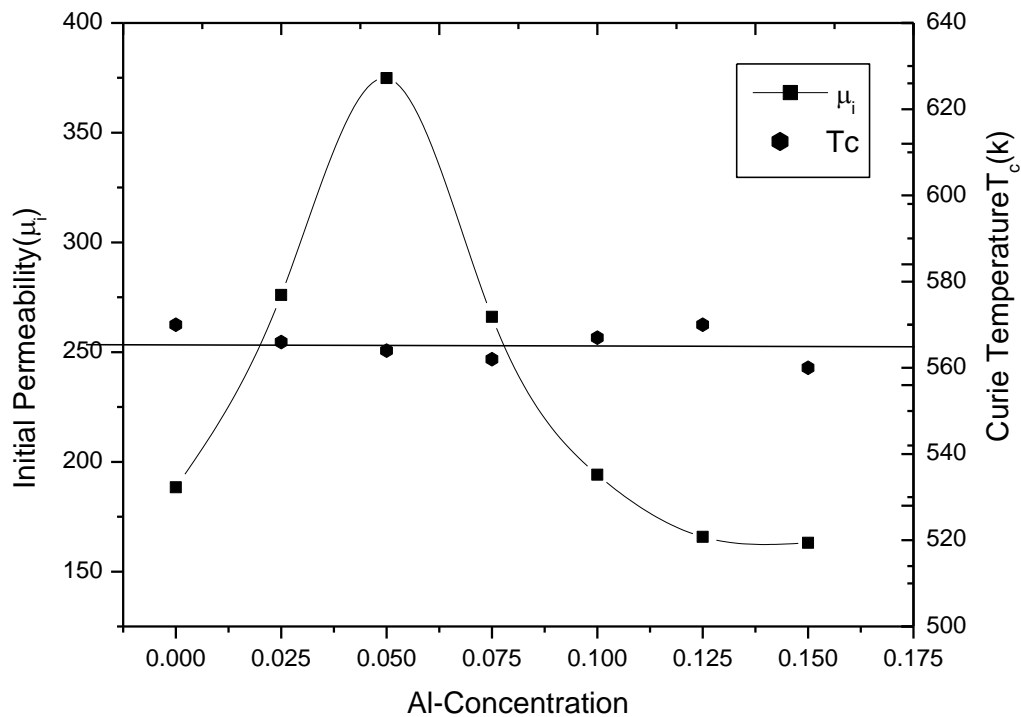


Fig.(6): Variation of initial permeability ( $\mu_i$ ) at room temperature and Curie temperature ( $T_c$ ) with Al-concentration

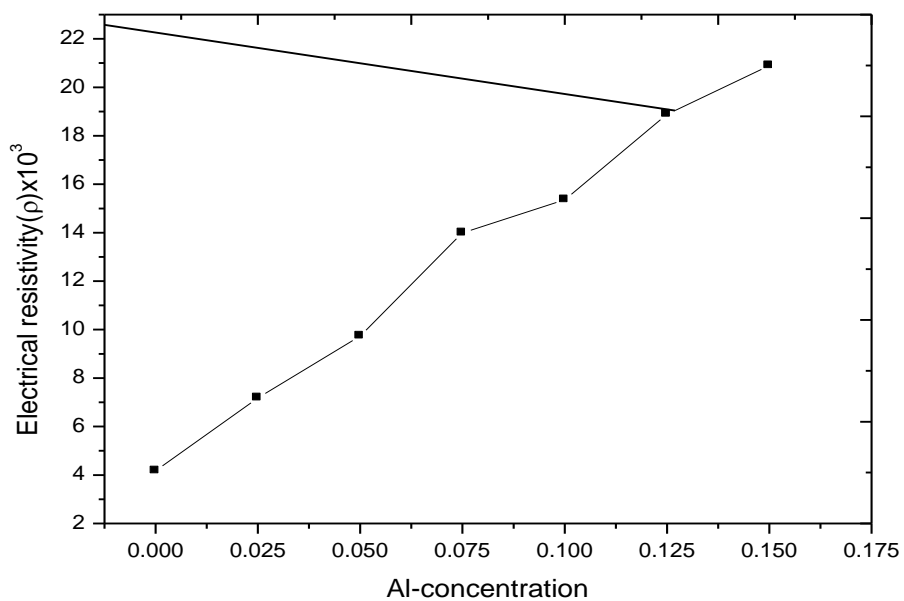




Fig.(7): The dependence of the electrical resistivity( $\rho$ ) at room temperature on Al-concentration

**Table (1):** Variation of D (nm), p (%),  $M_s$ (emu/g),  $\Delta M_s$ (%),  $\mu_i$ ,  $\Delta\mu_i$ (%) and  $\Delta\mu_i/\Delta T$  with Al-concentration(x).

Al-conc. (x)	Grain size D (nm)	Porosity P (%)	$M_s$ (emu/g)	$\Delta M_s$ (%)	$\mu_i$	$\Delta\mu_i$ (%)	$\Delta\mu_i/\Delta T$
0.00	56	3.7	77.1	---	190	---	6.1
0.025	293	6.3	81.2	5.1	276	45	8.9
0.05	350	9.5	82.5	6.9	374	96	12.7
0.075	255	8.4	82.3	6.7	267	40	7.9
0.10	130	6.8	77.2	0.1	193	1.4	4.2
0.125	108	5.4	72.1	-6.5	165	-13.2	3.9
0.15	98	5.3	71	-8	164	-13.7	4